J Therm Anal Calorim (2012) 108:865–870
DOI 10.1007/s10973-012-2387-2

Nano-crystalline $Mn_{0.3}Ni_{0.3}Zn_{0.4}Fe_2O_4$ obtained by novel fumarato-hydrazinate precursor method

Synthesis, characterization and studies of magnetic and electrical properties

U. B. Gawas · V. M. S. Verenkar · S. C. Mojumdar

CTAS2011 Conference Special Chapter

Abstract Carboxylate hydrazinate complex involving mixed metals have been synthesized and used as precursor for preparing the nanocrystalline Mn–Ni–Zn ferrite. Chemical composition of complex was fixed from chemical analysis results, infrared studies, thermogravimetric and differential scanning calorimetric analysis and isothermal weight loss studies. Nano-crystalline Mn–Ni–Zn ferrite particles obtained by thermal autocatalytic decomposition were characterized using X-ray diffraction studies, infrared spectral studies and TEM measurement. Two peaks in the region of 340–420 and 550–660 cm^{-1} observed in the infrared spectrum of "as synthesized" oxide are characteristics of spinel ferrites. Average particle size of "as synthesized" Mn–Ni–Zn ferrite was found to be 10 nm. "As synthesized" Mn–Ni–Zn ferrite showed Curie point at 313 °C. Saturation magnetization (44.7 emu/g) observed for "as synthesized" Mn–Ni–Zn ferrite is lower than bulk material which is indicative of its nano-crystalline nature. Seebeck coefficient measurement has shown that the material exhibits n-type semiconducting behavior.

U. B. Gawas · V. M. S. Verenkar
Department of Chemistry, Goa University,
Taleigao Plateau 403206, Goa, India

S. C. Mojumdar
Department of Chemical Technologies and Environment,
Faculty of Industrial Technologies, Trencin University
of A. Dubceck, Puchov, Slovakia

S. C. Mojumdar (✉)
Department of Chemistry, University of Guelph,
Guelph, ON, Canada
e-mail: scmojumdar@yahoo.com

Keywords Hydrazine complex · Nanoparticles · Spinel ferrite · TG · DSC · TEM

Introduction

Spinel ferrites are investigated in the recent years for their useful electrical and magnetic properties which find applications in information storage systems, magnetic bulk cores, magnetic fluids, microwave absorbers, and medical diagnostics [1]. Recently, the nano-crystalline ferrites are gaining more importance due to their unusual magnetic behavior and promising technological applications. Mn–Zn ferrites are widely used for magnetic application due to their high permeability and high magnetization [2]. Ni–Zn ferrites on the other hand possess high resistivity, but relatively low permeability at high frequencies [3]. For high frequency magnetic application ferrites with high permeability as well as high resistivity are needed. A combination of these two ferrites is envisaged to meet these requirements [4]. The magnetic and electrical properties of ferrites are sensitive to the cation distributions which in turn depend on method of synthesis. Various wet chemical methods like co-precipitation [5, 6], sol–gel [7–10] have been developed which are found to be superior over conventional ceramic method. Metal as well as mixed metal carboxylate complexes are found to be very good precursors for the synthesis of nano-crystalline metal as well as mixed metal oxides, as these precursors decomposes at comparatively lower temperatures [11, 12]. Coordination of hydrazine to the carboxylate was found to lower the decomposition temperature of metal carboxylate by providing the exothermicity [13]. Many such synthesis of metal oxides and mixed metal oxides using metal hydrazine complexes of oxalate [14, 15], glyoxylates

[16] sulfite [17], formate [18], acetate [19], malonate, succinate and itaconates [20–25], maleate [26] malate [27], and fumarate [26, 28–35] have been reported.

One such novel mixed metal hydrazine complex involving fumarate dianion is synthesized, characterized and successfully employed in the preparation of nano-crystalline $Mn_{0.3}Ni_{0.3}Zn_{0.4}Fe_2O_4$. The magnetic and electrical properties of "as synthesized" $Mn_{0.3}Ni_{0.3}Zn_{0.4}Fe_2O_4$ are also studied. As these ferrites are technologically important material extensively used in applications such as transformer core, noise filters, recording heads, etc. due to their high initial permeability and high saturation magnetization.

Experimental

Preparation of manganese nickel zinc ferrous fumarato–hydrazinate complex

The preparation method is similar to the earlier reported method [32]. The yellow precipitate obtained was filtered, washed with ethanol and dried with diethyl ether by suction. The dried precursor was stored in vacuum desiccators.

Characterization

The hydrazine content in the precursor was determined by volumetric analysis using standard 0.025 M KIO_3 solution under Andrew's conditions [36]. The metal content was determined by chemical analysis. The structure and phase purity of the manganese nickel zinc ferrite was determined on a Philips X-ray diffractometer model PW 3710 with Cu K_α radiations and Ni filter. Transmission electron micrograph analysis was carried out on a JEOL JEM 2100F electron microscope. Simultaneous thermogravimetric and differential thermal analysis of the precursor was recorded on NETZSCH DSC-TG STA 409PC at a heating rate of 10 °C per minute. Isothermal weight loss and total weight loss studies along with hydrazine analysis of the complex were carried out at various predetermined temperatures. Infrared spectral analysis of the complex and "as synthesized" ferrite was recorded on a FTIR Shimadzu IR Prestige 21 Series Spectrophotometer. The saturation magnetization of the as-synthesized powder was measured on alternating current hysteresis loop tracer described by Likhite et al. [37] and supplied by M/s Prutha Electronics, Mumbai, India. Curie temperature measurement was carried out from variation of magnetic moment as a function of temperature as describe by Likhite and Radhakrishnamurthy [38]. A dc resistivity measurement was carried out using two probe methods.

Autocatalytic decomposition of the precursor complex

Autocatalytic decomposition of the precursor was carried out spreading it uniformly in a ceramic tile and burning with splinter. When small portion catches fire, a red glow that formed spreads over the entire bulk completing the total decomposition of the precursor in an ordinary atmosphere to form ferrite at lower temperature. This "as synthesized" $Mn_{0.3}Ni_{0.3}Zn_{0.4}Fe_2O_4$ powder was heated at 400 °C for 5 h to remove any residual carbon formed during the decomposition of coordination complex and pelletized under a pressure of 7 tones per square inch for 3 min. Pellet of dimension 10 mm in diameter and 2 mm in thickness was used for measurement of magnetic and electrical properties.

Result and discussion

A chemical formula of $Mn_{0.3}Ni_{0.3}Zn_{0.4}Fe_2(C_4H_2O_4)_3 \cdot 6N_2H_4$ has been fixed based on the total percentage mass loss 66.66 % (66.60 %), percentage of hydrazine 27.22 % (27.24 %), manganese 2.30 % (2.33 %), nickel 2.45 % (2.49 %), zinc 3.65 % (3.70 %), and iron 15.82 % (15.82 %) which match closely with the calculated values given in the parenthesis (Table 1) considering above composition. The infrared spectra of the precursor (Fig. 1) show three bands in the region 3,167–3,352 cm^{-1} which are characteristics of N–H stretching and in the range of 1,552–1,585 cm^{-1} which are due to NH_2 deformation. The N–N stretching frequency is observed at 977 cm^{-1} which confirms the bidentate bridging nature of hydrazine ligand [39, 40]. The asymmetric and symmetric stretching frequencies of the carboxylate ion in the precursor are observed at 1624 and 1385 cm^{-1}, respectively, with separation $\Delta\nu$ ($\nu_{asy}-\nu_{sym}$) of 239 cm^{-1} indicating the monodentate linkage of both carboxylate groups in the dianions [41]. Thus, the fumarate dianion coordinate to the metal as bidentate ligand in the complex. These results supports the formation of $Mn_{0.3}Ni_{0.3}Zn_{0.4}Fe_2(C_4H_2O_4)_3 \cdot 6N_2H_4$ complex. Besides thermogravimetry,

Table 1 Chemical and thermal analysis of manganese nickel zinc ferrous fumarato-hydrazinate, $Mn_{0.3}Ni_{0.3}Zn_{0.4}Fe_2(C_4H_2O_4)_3 \cdot 6N_2H_4$

Precursor complex	Mn/%		Ni/%		Zn/%		Fe/%		N_2H_4/%		Total mass loss/%	
	Obs	Calc.	Obs	Calc.	Obs	Calc.	Obs	Calc.	Obs	Calc.	Obs	Calc.
$Mn_{0.3}Ni_{0.3}Zn_{0.4}Fe_2$ $(C_4H_2O_4)_3 \cdot 6N_2H_4$	2.30	2.33	2.45	2.49	3.68	3.70	15.82	15.82	27.24	27.22	66.66	66.60

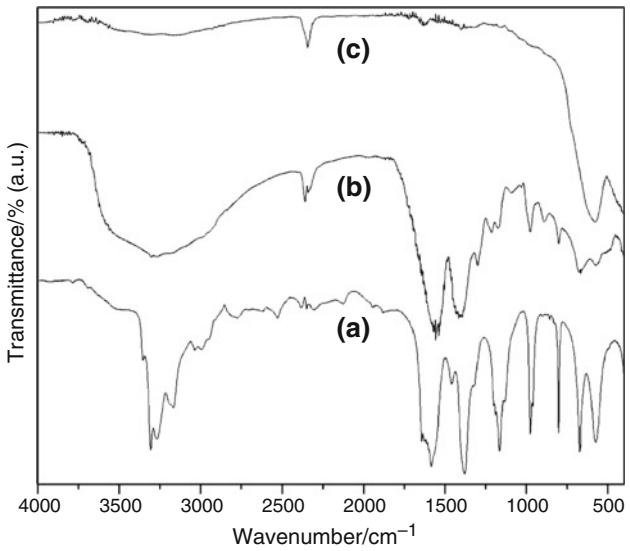

Fig. 1 IR spectrum of (*a*) Hyrazinated precursor, (*b*) Dehydrazinated Precursor (heated at 170 °C), and (*c*) Decomposed product

thermal decomposition of the complex was also studied using infrared spectroscopy by carefully heating the precursor at the rate of 4 °C per minute. Infrared spectra of the precursor heated at 170 °C shows no peaks in the region which corresponds to the N–H stretching instead a broad band is observed in this region which may be due to the simultaneous hydration of the complex after dehydrazination (Fig. 1b). This observation suggests the complete dehydrazination of the complex occurs at 170 °C which was also confirmed by chemical analysis and isothermal weight loss studies. It has also been observed that the presence of hydrazine is must for these complexes to exhibit self propagating combustion behavior since dehydrazinated complex do not show such behavior (Table 2).

Thermal analysis and phase identification of decomposed product

The TG curve (Fig. 2) of $Mn_{0.3}Ni_{0.3}Zn_{0.4}Fe_2(C_4H_2O_4)_3 \cdot 6N_2H_4$ complex in air from room temperature to 800 °C shows four mass loss regions with three major ones. Initial mass loss of around 1.45 % till 60 °C corresponds to the adsorbed moisture on the complex indicated by small endothermic peak which is also reflected in the infrared spectrum of the complex wherein weak absorption band is observed in the region 3,400–3,600 cm^{-1}. The mass loss of 15.85 % from 60 to 100 °C corresponds to the loss of three and half hydrazine molecules. The mass loss of about 15.21 % in the TG curve from 100 to 170 °C corresponds to the loss of two and half hydrazine molecules and complete dehydrazination which was confirmed from isothermal mass loss studies and infrared spectrum (Fig. 1b). The decomposition of dehydrazinated fumarato complex begins simultaneously with dehydrazination and major mass loss of 31.07 % in thermogravimetric measurement from 170 to 350 °C is attributed to the decarboxylation of the dehydrazinated complex. DSC analysis shows (Fig. 2) two sharp exothermic peaks at 87.2 and 165.3 °C due to two step dehydrazination and a sharp exothermic peak at 294.8 °C corresponds to the one-step oxidative decarboxylation. A marginal mass loss of 3.45 % in the region 350–420 °C may be due to unburned carbon which is indicated in the DSC by a broad exothermic peak in this region. The complex decomposes autocatalytically at room temperature, once ignited, to give nanocrystalline $Mn_{0.3}Ni_{0.3}Zn_{0.4}Fe_2O_4$ (as synthesized). X-ray diffraction pattern (Fig. 3) indicates the formation of single phase spinel ferrite and broadness of peaks indicates the nanocrystalline nature of $Mn_{0.3}Ni_{0.3}Zn_{0.4}Fe_2O_4$. The IR spectra of the "as synthesized" $Mn_{0.3}Ni_{0.3}Zn_{0.4}Fe_2O_4$ (Fig. 1c) show high frequency ν_1 at 574.8 cm^{-1} and low frequency ν_2 bands at 405 cm^{-1} which corresponds the metal–oxygen stretching tetrahedral and octahedral sites in spinel structure supporting the formation of single-phase $Mn_{0.3}Ni_{0.3}Zn_{0.4}Fe_2O_4$ [42, 43]. The TEM (Fig. 4) shows the uniform distribution of particles with average particle size 10 nm confirming the nano-crystalline nature of "as synthesized" $Mn_{0.3}Ni_{0.3}Zn_{0.4}Fe_2O_4$. The plot of magnetic moment on temperature (Fig. 5) indicates that the sample contains single domain particles with a curie temperature of 313 °C.

Table 2 TG-DSC, isothermal mass loss and chemical analysis data of $Mn_{0.3}Ni_{0.3}Zn_{0.4}Fe_2(C_4H_2O_4)_3 \cdot 6N_2H_4$ complex

TG		DSC peak/°C	Remarks	Isothermal mass loss studies		
Temp. range/°C	Mass loss/%			Temp. range/°C	Weight loss/%	N_2H_4/%
RT-60	1.45	55 (Endo)	Loss of adsorbed moisture	RT-60	1.42	27.26
60–100	15.85	87.2 (Exo)	Loss of three and half N_2H_4 molecule	70–100	4.62	22.57
100–170	15.21	184.7 (Exo)	Loss of two and half N_2H_4 molecule and decarboxylation	100–130	9.78	13.42
170–340	31.07	294.8 (Exo)		130–150	7.52	6.45
340–420	3.58	340–420 (Exo)		150–170	6.43	–

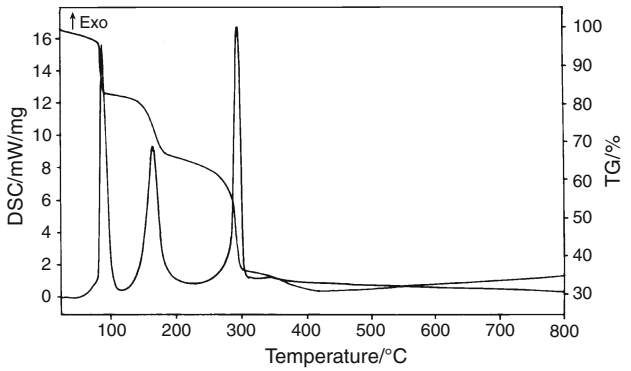

Fig. 2 TG-DSC curves of $Mn_{0.3}Ni_{0.3}Zn_{0.4}Fe_2(C_4H_2O_4)_3{\cdot}6N_2H_4$ complex

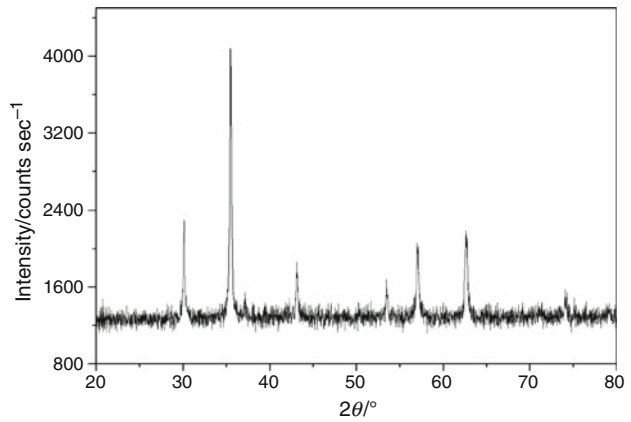

Fig. 3 XRD pattern of "as synthesized" of $Mn_{0.3}Ni_{0.3}Zn_{0.4}Fe_2O_4$

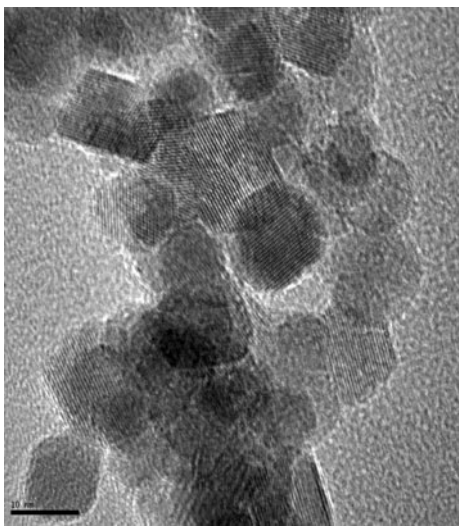

Fig. 4 TEM of "as synthesized" $Mn_{0.3}Ni_{0.3}Zn_{0.4}Fe_2O_4$

Saturation magnetization of "as synthesized" $Mn_{0.3}Ni_{0.3}Zn_{0.4}Fe_2O_4$ was found to be 44.7 emu/g, which is lower than the normally expected higher for bulk

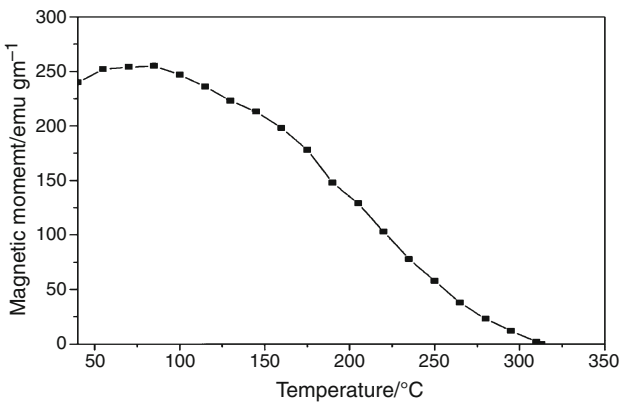

Fig. 5 Plot of magnetic moment versus temperature/°C

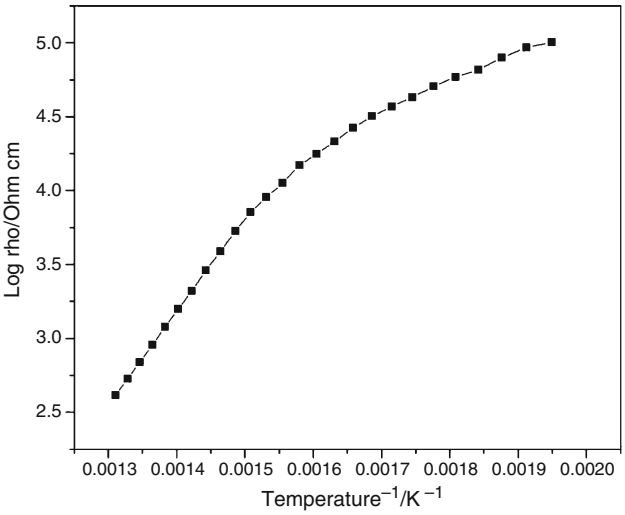

Fig. 6 Plot of log resisistivity versus temperature^{-1}/K^{-1}

$Mn_{0.3}Ni_{0.3}Zn_{0.4}Fe_2O_4$. The reason for the lower value of saturation magnetization is the high porosity and the small particle size of "as synthesized" $Mn_{0.3}Ni_{0.3}Zn_{0.4}Fe_2O_4$. The variation of electrical resistivity versus temperature (Fig. 6) shows decrease in resistivity with increasing temperature, as expected. The plot shows change in the slope at 315 °C due to the switching of the magnetic region from ferrimagnetic to paramagnetic which is in accordance with the literature reports [44]. The variation of Seebeck coefficient as a function of temperature shows a negative sign of thermo-emf suggesting the material is n-type semiconductor.

Conclusions

- $Mn_{0.3}Ni_{0.3}Zn_{0.4}Fe_2(C_4H_2O_4)_3{\cdot}6N_2H_4$ complex was prepared for the first time and successfully employed to obtained nano-crystalline $Mn_{0.3}Ni_{0.3}Zn_{0.4}Fe_2O_4$ at relatively lower temperatures.

- The formation of single phase $Mn_{0.3}Ni_{0.3}Zn_{0.4}Fe_2O_4$ was confirmed by X-ray diffraction as well as infrared spectral studies.
- The average particle size of "as synthesized" $Mn_{0.3}Ni_{0.3}Zn_{0.4}Fe_2O_4$ was found to be 10 nm as shown by TEM analysis.
- "As synthesized" $Mn_{0.3}Ni_{0.3}Zn_{0.4}Fe_2O_4$ has shown the lower value of saturation magnetization as compared to their bulk counterpart because of its nano-crystalline nature.
- Curie temperature of "as synthesized" $Mn_{0.3}Ni_{0.3}Zn_{0.4}Fe_2O_4$ was found to be in the range 313–315 °C as determine from magnetic susceptibility and dc resistivity measurement.
- Seebeck coefficient measurement of "as synthesized" $Mn_{0.3}Ni_{0.3}Zn_{0.4}Fe_2O_4$ displays n-type semiconducting behavior.

Thus, this study confirms that nano-crystalline $Mn_{0.3}Ni_{0.3}Zn_{0.4}Fe_2O_4$ can be synthesize easily using fumarato–hydrazinate complex of mixed metals as precursor, at comparatively lower temperatures. This material finds applications in transformer cores used in power supplies which are an integral part of almost every electronic equipments.

References

1. Mathew DS, Juang RS. An overview of the structure and magnetism of spinel ferrite nanoparticles and their synthesis in microemulsions. Chem Eng J. 2007;129:51–65.
2. Singh AK, Singh AK, Goel TC, Mendiratta RG. High performance Ni-substituted Mn–Zn ferrites processed by soft chemical technique. J Magn Magn Mater. 2004;281:276–80.
3. Goldman A. Modern ferrite technology. 2nd ed. New York: Wiley; 1990. p. 71.
4. Singh AK, Verma A, Thakur OP, Prakash C, Goel TC, Mendiratta RG. Electrical and magnetic properties of Mn–Ni–Zn ferrites processed by citrate precursor method. J Magn Magn Mater. 2003;57:1040–4.
5. Venkatraju C, Sathishkumar G, Sivakumar K. Effect of cation distribution on the structural and magnetic properties of nickel substituted nanosized Mn–Zn ferrites prepared by co-precipitation method. J Magn Magn Mater. 2010;322:230–3.
6. Jadhav SS, Shirsath SE, Toksha BG, Shukla SJ, Jadhav KM. Effect of cation proportion on the structural and magnetic properties of Ni–Zn Ferrites nano-size particles prepared by co-precipitation technique. Chin J Chem Phys. 2008;21(4):381–6.
7. Verma A, Chatterjee R. Effect of zinc concentration on the structural, electrical and magnetic properties of mixed Mn–Zn and Ni–Zn ferrites synthesized by citrate precursor technique. J Magn Magn Mater. 2006;306:313–20.
8. Singh AK, Goel TC, Mendiratta RG. Effect of cation distribution on the properties of $Mn_{0.2}Zn_xNi_{0.8-x}Fe_2O_4$. Solid State Comm. 2003;12:121–5.
9. Bueno AR, Gregori ML, Nobrega MCS. Microwave absorbing properties of $Ni_{0.5-x}Zn_{0.5-x}Me_{2x}Fe_2O_4$(Me = Cu, Mn, Mg) ferrite–wax composite in X-band frequencies. J Magn Magn Mater. 2008;320:864–70.
10. Stefanescu M, Stoia M, Stefanescu O, Barvinshi P. Obtaining of $Ni_{0.65}Zn_{0.35}Fe_2O_4$ nanoparticles at low temperature starting from metallic nitrates and polyols. J Therm Anal Calorim. 2010; 99(2):459.
11. Deb N. Thermal decomposition of manganese (II) bis(oxalato) nickelate(II) tetrahedrate. J Therm Anal Calorim. 2005;81:61–5.
12. Carp O, Patron L, Pascu G, Mindru L, Stanica N. Thermal investigations of nickel–zinc ferrites formation from malate coordination compounds. J Therm Anal Calorim. 2006;84(2): 391–4.
13. Rane KS, Uskaikar H, Pednekar R, Mhalsikar R. The low temperature synthesis of metal oxides by novel hydrazine method. J Therm Anal Calorim. 2007;90(3):627–38.
14. Rane KS, Verenkar VMS. Synthesis of ferrite grade γ-Fe_2O_3. Bull Mater Sci. 2001;24(1):39–45.
15. Gajapathy D, Patil KC, Pai Vernekar VR. Low temperature ferrite formation using metal oxalate hydrazinate precursor. Mat Res Bull. 1982;17(1):29–32.
16. Raju B, Sivasankar BN. Spectral, thermal and X-ray studies on some new bis hydrazine lanthanide(III) glyoxylates. J Therm Anal Calorim. 2008;94(1):289–96.
17. Budkuley JS, Patil KC. Synthesis and thermoanalytical properties of mixed metal sulfite hydrazinate hydrates II. Synth React Inorg Met Org Chem. 1991;21(4):709–15.
18. Ravindranathan P, Patil KC. Thermal reactivity of metal formate hydrazinates. Thermochim Acta. 1983;71:53–7.
19. Mahesh GV, Patil KC. Thermal reactivity of metal acetate hydrazinates. Thermochim Acta. 1986;99(1):153–8.
20. Randhawa BS, Dosanjh HS, Kumar N. Synthesis of potassium ferrite by precursor and combustion methods a comparative study. J Therm Anal Calorim. 1999;95(1):75–80.
21. Sivasankar BN, Govindarajan S. Studies on bis(hydrazine) metal malonates and succinates. Synth React Inorg Met Org Chem. 1994;24(9):1573–82.
22. Sivasankar BN. Cobalt(II), nickel(II) and zinc(II) dicarboxylate complexes with hydrazine as bridged ligand characterization and thermal degradation. J Therm Anal Calorim. 2006;86(2):385–92.
23. Sivasankar BN, Govindarajan S. Hydrazine mixed metal malonates—new precursors for metal cobaltites. Mater Res Bull. 1996; 31(1):47–54.
24. Sivasankar BN, Govindrajan S. Acetate and malonate complexes of cobalt (II), nickel(II) and zinc(II) with hydrazinium cation: preparation, spectral and thermal studies. J Therm Anal. 1997; 48(6):1401–13.
25. Verenkar VMS, Porob RA, Sawant SY, Kannan KR. Synthesis, characterisation and thermal analysis of nickel manganese succinato-hydrazinate. In: Singh Mudher KD, Bharadwaj S, Ravindran PV, Sali SK, Venugopal V, editors. Proceedings of the 14th national symposium on thermal analysis, Thermans 2004. Vadodara: Indian Thermal Analysis Society; 2004. p. 335–337.
26. Govindrajan S, Banu SUN, Sarayanan N, Sivasankar BN. *Bis*-hydrazine metal maleate and fumarate: preparation, spectral and thermal studies. Proc Indian Acad Sci (Chem Sci). 1995;107(5): 559–65.
27. Khalil I, Petit-Ramel MM. Polynuclear complexes quantitative and qualitative study of copper-yttrium malate and copper-uranyl malate. J Inorg Nucl Chem. 1979;41(5):711–6.
28. Porob RA, Khan SZ, Mojumdar SC, Verenkar VMS. Synthesis, TG, DSC and infrared spectral study of $NiMn_2(C_4H_4O_4)_3{\cdot}6N_2H_4$: a precursor for $NiMn_2O_4$ nanoparticles. J Therm Anal Calorim. 2006;86(3):605–8.
29. Gawas U, Bhattacharya S, More A, Verenkar VMS. Synthesis and characterization of $Ni_{0.6}Zn_{0.4}Fe_2O_4$ obtained by self propagating auto-combustion of a novel precursor. In: Lokhande CD, editor. Proceedings of the international conference on advanced materials and applications. Kolhapur; 2007. p. 86–93.

30. Sawant SY, Verenkar VMS, Mojumdar SC. Preparation, thermal, XRD, chemical and FTIR spectral analysis of $NiMn_2O_4$ nanoparticles and respective precursor. J Therm Anal Calorim. 2007; 90(3):669–72.
31. More A, Verenkar VMS, Mojumdar SC. Nickel ferrite nanoparticles synthesis from novel fumarato-hydrazinate precursor. J Therm Anal Calorim. 2008;94(1):63–7.
32. Gawas UB, Mojumdar SC, Verenkar VMS. $Ni_{0.5}Mn_{0.1}Zn_{0.4}Fe_2(C_4H_2O_4)_3{\cdot}6N_2H_4$ precursor $Ni_{0.5}Mn_{0.1}Zn_{0.4}Fe_2O_4$ nanoparticles preparation, IR spectral, XRD, SEM-EDS and thermal analysis. J Therm Anal Calorim. 2009;96(1):49–52.
33. Gonsalves LR, Verenkar VMS, Mojumdar SC. Preparation and characterization of $Co_{0.5}Zn_{0.5}Fe_2(C_4H_2O_4)_3{\cdot}6N_2H_4$: a precursor to prepare $Co_{0.5}Zn_{0.5}Fe_2O_4$ nanoparticles. J Therm Anal Calorim. 2009;96(1):53–7.
34. Gawas UB, Mojumdar SC, Verenkar VMS. Synthesis, characterization, infrared studies, and thermal analysis of $Mn_{0.6}Zn_{0.4}Fe_2(C_4H_2O_4)_3{\cdot}6N_2H_4$ and its decomposition product $Mn_{0.6}Zn_{0.4}Fe_2O_4$. J Therm Anal Calorim. 2010;100(3):867–71.
35. Gonsalves LR, Mojumdar SC, Verenkar VMS. Synthesis of cobalt nickel ferrite nanoparticles via autocatalytic decomposition of the precursor. 2010;100(3):789–92.
36. Vogel's, Text book of quantitative inorganic analysis (Revised by Jeffery GH, Bassettv, Mendham J and Denney RC). 5th ed. Longman; 1989. p. 402.
37. Likhite SD, Radhakrishnamurthy C, Sahasrabudhe PW. Alternating current electromagnet type hysteresis loop tracer for minerals and rocks. Rev Sci Instr. 1965;36(11):1558–60.
38. Likhite SD, Radhakrishnamurthy C. Initial susceptibility and constricted rayleigh loops of some basalts. Curr Sci. 1966;35: 534–6.
39. Braibanti A, Dallavalle F, Pellinghelli MA, Leporati E. The nitrogen–nitrogen stretching band in hydrazine derivatives and complexes. Inorg Chem. 1968;7:1430–3.
40. Tsuchiya R, Yonemura M, Uehera A, Kyuno E. Derivatographic studies on transition metal complexes. XIII. Thermal decomposition of $[Ni(N_2H_4)_6]X_2$ complexes. Bull Chem Soc Jpn. 1974;47(3): 660–4.
41. Nakamoto K. Infrared and Raman spectra of inorganic and coordination compounds part B. 6th ed. New York: Wiley; 1978. p. 13.
42. Waldron RD. Infrared spectra of ferrites. Phys Rev. 1955;99: 1727–35.
43. Srinivasan TT, Srivastava CM, Venkataramani N, Patni MJJ. Infrared absorption in spinel ferrites. Bull Mater Sci. 1984;6(6): 1063–7.
44. Peng CH, Hwang CC, Hongb CK, Chen SY. A self-propagating high-temperature synthesis method for Ni-ferrite powder synthesis. Mater Sci Eng B. 2004;107:295–300.